Room-temperature scintillation properties of cerium-doped REOX (RE=Y, La, Gd, and Lu; X=F, Cl, Br, and I)

Yetta D. Eagleman[a], Edith Bourret-Courchesne[a] and Stephen E. Derenzo[a]

[a] Lawrence Berkeley National Laboratory, Berkeley, CA 94720, USA

Received 25 July 2010;
revised 9 November 2010;
accepted 14 November 2010.
Available online 20 November 2010.

Abstract

The scintillation properties of cerium-doped oxyhalides following the general formula REOX (RE=Y, La, Gd, and Lu; X=F, Cl, Br, and I) are reported. These materials were synthesized under dry conditions as microcrystalline powders from conventional solid state reactions. The room temperature X-ray excited emission and scintillation decay curves were measured and analyzed for each material. Additionally, the hygroscopic nature of the oxychlorides and oxybromides was compared to that of their corresponding rare earth halides. The yttrium, lanthanum, and gadolinium oxychlorides, and all of the oxybromides and oxyiodides are found to be activated by Ce^{3+}. GdOBr doped with 0.5% Ce^{3+} has the highest light output with a relative luminosity of about one-half that of $LaBr_3$: Ce^{3+}. It displays a single exponential decay of 30 ns.

Research Highlights

►Room temperature scintillation properties of cerium doped rare earth oxyhalides. ►Oxybromides and oxyiodides most efficient scintillators. ►Cerium activation may be linked to structure.

Keywords: Scintillator; Cerium; Oxyhalides; Luminescence

1. Introduction

Cerium-doped rare earth halides display desirable [1] high scintillation light yields with fast decay components [2], [3], [4], [5], [6], [7], [8], [9], [10] and [11] (e.g., $LaBr_3$: Ce^{3+} has been reported to have luminosities in the range of 61,000–74,000 phs/MeV and decay times <40 ns , [6] and [10]), and hence they have garnered much attention. Though these halides are attractive scintillators, their hygroscopic nature make them difficult to handle. Traditionally, metal oxide scintillators are more air stable.

In this work, we investigated inorganic hosts containing both oxide and halide ions in an attempt to discover new host materials that are more stable than the rare earth halides and have comparable scintillation properties when doped with cerium. Yttrium, lanthanum, gadolinium, and lutetium oxychlorides and oxybromides doped with trivalent cerium have been previously studied for use in

cathodoluminescent and X-ray intensifying screens [12], [13], [14] and [15]. Here we report the scintillation properties (emission spectra, decay curves, and decay times) of these materials and added those of the oxyfluorides and oxyiodides, following the general formula REOX (RE=Y, La, Gd, and Lu; X=F, Cl, Br, and I). Relative luminosities are obtained by normalization to the known scintillator $LaBr_3$: 5% Ce^{3+}. A semi-quantitative study is included of the chemical stability of the oxychlorides and oxybromides.

2. Experimental

2.1. Synthesis

The oxyfluoride and oxyiodide materials were produced from the solid state reaction

$$RE_2O_3(s) + REX_3(s) \rightarrow 3REOX(s) \quad (RE = Y, La, Gd, \text{ and } Lu; X = F \text{ and } I) \tag{1}$$

Finely ground mixtures of the rare earth oxides and fluorides were reacted in capped alumina tubes under 3% H_2/argon flow at 1000 °C for 10 h. The oxyiodides were synthesized at the same temperature and duration in sealed evacuated quartz tubes. The rare earth iodides and the oxyiodide products are sensitive to light and moisture; therefore, all manipulations of these materials were performed in the dark in an argon-filled glove box.

The rare earth oxychlorides and oxybromides were synthesized in accordance with

$$RE_2O_3(s) + 2NH_4X(s) \rightarrow 2REOX(s) + 2NH_3(g) + H_2O(g) \quad (RE = Y, La, Gd, \text{ and } Lu; X = Cl \text{ and } Br) \tag{2}$$

where mixtures of the corresponding rare earth oxide and ammonium chloride or bromide (1:2 molar ratio) were reacted under 3% H_2/argon flow following a modified synthesis procedure of [16] and [17]. Each mixture was initially heated at 450 °C for 1 h, allowing the release of ammonia and water gases. Subsequently, the temperature was raised to 800 °C and was held there for 1 h to crystallize the phases.

Each REOX material was prepared in its undoped and doped forms. Concentrations of 0.5, 1, 2, 5, and 10 mole% of the rare earth precursors were replaced by cerous oxide (Ce_2O_3) and/or cerium halide (CeX_3). With the exception of the oxyiodides, all oxyhalides are colorless hygroscopic powders. The oxyiodides are hygroscopic and tan.

2.2. Characterization

Proper synthesis of each material was confirmed by powder X-ray diffraction. The diffractometer is an in-house diffraction setup utilizing a Bruker Nonius FR591 rotating anode X-ray generator operated at 50 kV and 60 mA. A more detailed description of this setup is supplied in [17].

Once the structure of each material was confirmed, a quantitative test was taken of the hygroscopic nature of the undoped oxychlorides and oxybromides. The weight gain for ~100 mg of each sample

was recorded at room temperature in open air (75% humidity) over 95 h. Identical measurements were conducted on the corresponding rare earth halides for comparison.

Room temperature X-ray excited luminescence spectra and pulsed X-ray decay curves were measured for each REOX and $LaBr_3$: 5% Ce^{3+} microcrystalline powder in sealed quartz cuvettes. Details of these procedures can be found in [18] and [19]. Multiple high-statistics pulsed X-ray data sets were used to determine the standard deviations in the decay times. For each material a minimum of four replicate data sets were acquired, and each contained typically 4 million events. A sum of exponential decay components was fit to each data set. In all cases the same components were identified with exponential decay times that differed somewhat due to the statistical fluctuations in the data.

The total luminosities were determined from pulsed X-ray measurements by summing all detected photons. Relative luminosities of each sample, RL_{Sample}, were calculated by

$$RL_{Sample} = \frac{PL_{Sample}}{PL_{Stnd}} \quad (3)$$

where PL_{Sample} and PL_{Stnd} are the luminosities obtained for the sample and standard, $LaBr_3$: 5% Ce^{3+}, powders, respectively.

3. Results

3.1. Physical properties

3.1.1. Densities and Z_{eff}

The densities and Z_{eff} of the REOX (RE=Y, La, Gd, and Lu; X=F, Cl, Br, and I) compounds are listed in Table 1. These physical parameters are important determinates of the stopping power of a scintillator [1]. The higher the density and Z_{eff} of a host, the better the material will absorb ionizing radiation. The compounds studied have densities and Z_{eff} comparable to $LaBr_3$ (ρ=5.1 g/cm^3; Z_{eff}=47).

Table 1. Physical and scintillation properties of cerium-doped REOX (RE=Y, La, Gd, and Lu; X=F, Cl, Br, and I) at their optimized cerium concentrations.

Compound	Crystal system [19]	Density	Z_{eff}[a]	Ce^{3+} doping (mole%)	Emission wavelength (nm)	Luminosity relative to $LaBr_3$: 5% Ce^{3+}[b]	Major decay times (≥10% of light)
YOF	Rhombohedral [20]	5.23	36	0.5	330, 400	<0.01	1906±9 (77%)
LaOF	Rhombohedral [21]	6.03	47	2	490	<0.01	2058±30 (36%)
GdOF	Rhombohedral [22]	7.69	49	0.5	–	<0.01	1405±417 ns (16%)

Compound	Crystal system [19]	Density	Z_{eff}[a]	Ce^{3+} doping (mole%)	Emission wavelength (nm)	Luminosity relative to $LaBr_3$: 5% Ce^{3+}[b]	Major decay times (≥10% of light)
LuOF	Monoclinic [23]	–	51	1	–	<0.01	80±6 (16%); 335±16 (16%); 1882±91 (23%)
YOCl	Tetragonal [24]	4.64	35	1	380	0.05	20±0 ns (83%)
LaOCl	Tetragonal [25]	5.45	45	2	420	<0.01	17±1 ns (15%); 106±5 ns (16%); 836±18 ns (15%);
GdOCl	Tetragonal [24]	6.66	48	0.5	400	0.25	Rise time: 6±1 ns; 25±1 ns (63%); 76±13 ns (27%)
LuOCl	Rhombohedral [26]	7.16	51	0.5	380	0.08	377±24 ns (16%); 1512±10 ns (77%)
YOBr	Tetragonal [19]	5.06	36	1	400, 445	0.15	25±0 ns (76%); 59±2 ns (17%)
LaOBr	Tetragonal [25]	6.17	47	1	425	0.04	1±0 ns (11%); 4±0 ns (26%); 13±0 ns (35%)
GdOBr	Tetragonal [27]	6.82	49	0.5	405, 445	0.49	Rise time: 10±1 ns; 30±1 ns (100%)
LuOBr	Tetragonal[19]	7.58	52	0.5	405, 445	0.10	25±0 ns (56%); 73±1 ns (10%)
YOI	Tetragonal [19]	5.42	48	1	430, 480	0.07	23±0 ns (85%)
LaOI	Tetragonal [25]	5.91	54	2	470	0.11	24±0 ns (86%)
GdOI	Tetragonal [28]	6.85	56	2	440, 470	0.10	23±0 ns (67%)

Compound	Crystal system [19]	Density	Z_{eff}[a]	Ce^{3+} doping (mole%)	Emission wavelength (nm)	Luminosity relative to $LaBr_3$: 5% Ce^{3+}[b]	Major decay times (≥10% of light)
LuOI	Tetragonal [29]	7.71	59	1	430, 480	0.01	23±0 ns (82%); 73±1 ns (10%)

[a] Z_{eff} is calculated by (4), $Z_{eff} = (W_A Z_A^4 + W_B Z_B^4 + W_C Z_C^4)$ (4) where W_A, W_B, W_C, Z_A, Z_B, and Z_C are the weight ratios and atomic numbers of elements A, B, and C, respectively [30].

[b] Relative luminosities calculated utilizing (3).

3.1.2. Hygroscopic nature

The increase in weight of the rare earth halides and oxyhalides while sitting in an open container exposed to open air is attributed to their absorption of moisture. After 95 h, the percentage of weight gained by the rare earth oxyhalides was less than a third of the weight gained by the rare earth halides (Fig. 1(a) and (b)). The hygroscopic nature of each rare earth oxyhalide is inversely related to the ionic size of their rare earth. The ionic radii of these trivalent cations (*CN*=8) follow the trend: Lu^{3+} (0.98 Å)<Y^{3+} (1.02 Å)≈Gd^{3+} (1.05 Å)<La^{3+} (1.22 Å) [31]. Likewise, their hygroscopic natures follow a similar trend in which the smaller the rare earth, the more hygroscopic the material. The oxyfluorides and oxyiodides were excluded from these experiments; the fluorides tend to be stable and the iodides are light sensitive, making them less viable as useful scintillators.

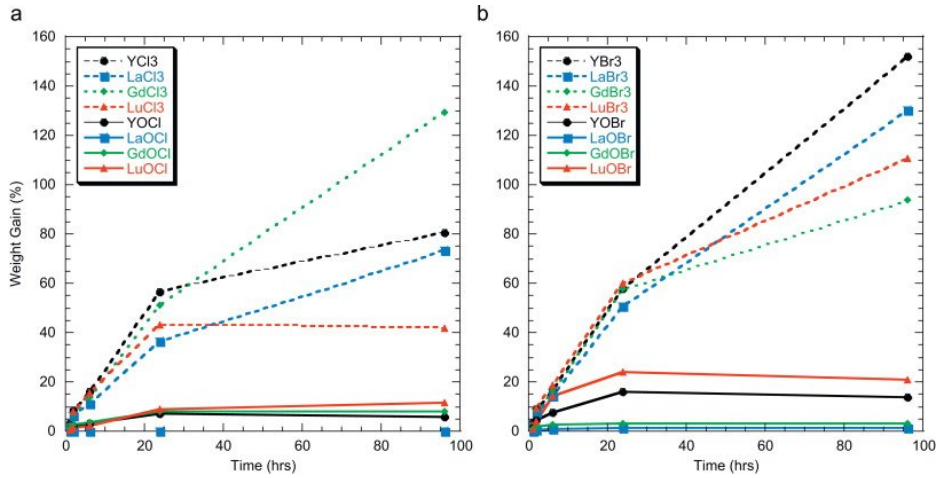

Fig. 1. (a and b) Hygroscopic nature (moisture absorption) of REX_3 and REOX, where RE=Y, La, Gd, and Lu, and (a) X=Cl and (b) X=Br.

3.2. Luminescence properties

X-ray excited emission spectra and pulsed X-ray decay curves were obtained for each undoped and cerium-doped REOX sample. A repeatable luminosity value for each material was achieved within 10%. Attention was given to changes in luminosities, emission peak maxima, and decay curve structures with variation of cerium concentration. Table 1 lists the emission peak maxima and major decay times found for each cerium-doped REOX material at the concentration that produced the highest light yield. The averages and standard deviations of the fitted decay times are listed. The standard deviations of the fitted fractions of the exponential components were typically 0.01 and less than 0.02 in all cases. Select X-ray excited emission spectra and decay curves are presented in Fig. 2(a–h).

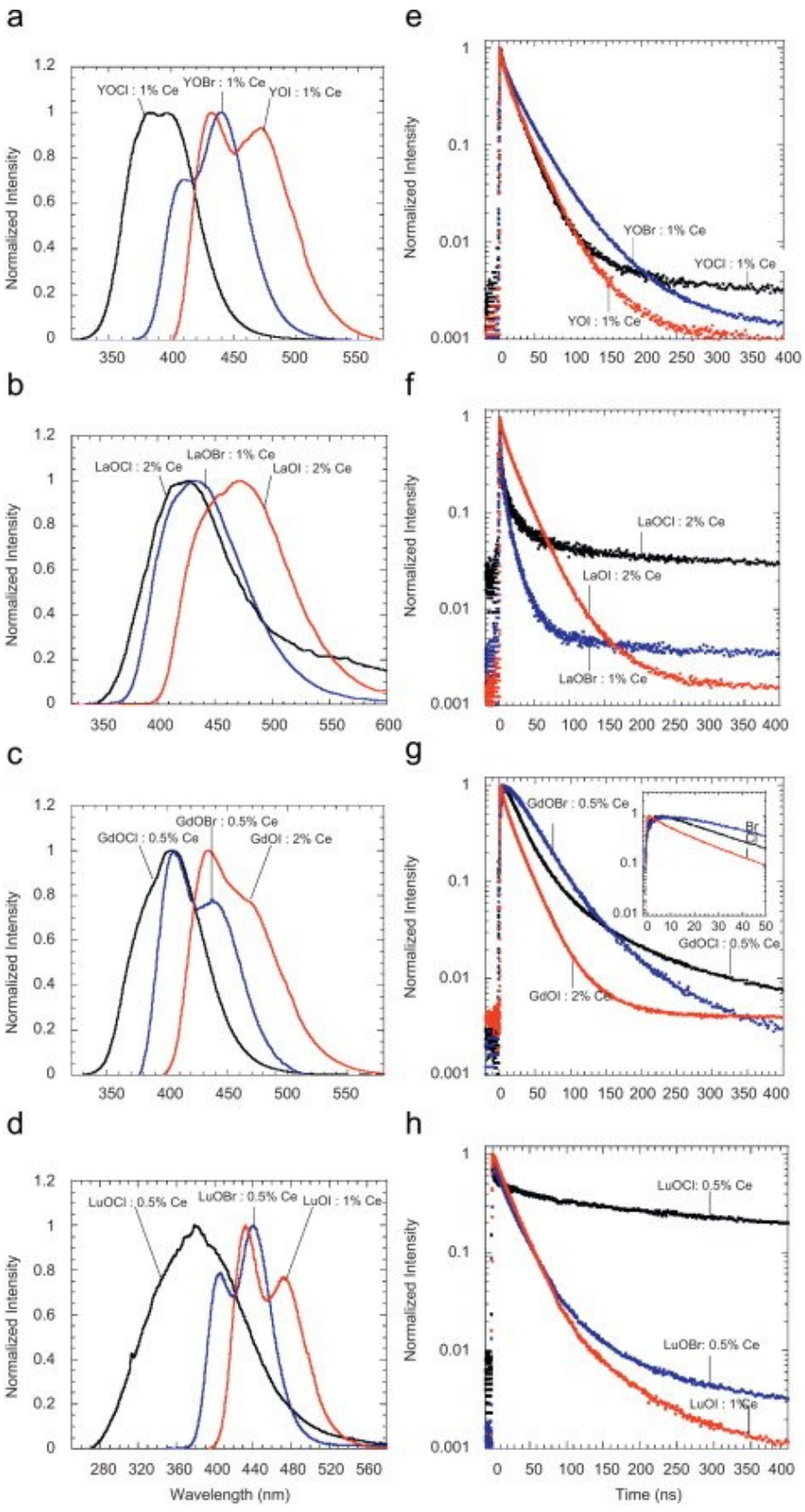
a
YOCl : 1% Ce
YOBr : 1% Ce
YOI : 1% Ce
Normalized Intensity
b
LaOCl : 2% Ce
LaOBr : 1% Ce
LaOI : 2% Ce
c
GdOCl : 0.5% Ce
GdOBr : 0.5% Ce
GdOI : 2% Ce
d
LuOCl : 0.5% Ce
LuOBr : 0.5% Ce
LuOI : 1% Ce
Wavelength (nm)
e
YOBr : 1% Ce
YOCl : 1% Ce
YOI : 1% Ce
f
LaOCl : 2% Ce
LaOI : 2% Ce
LaOBr : 1% Ce
g
GdOBr : 0.5% Ce
GdOCl : 0.5% Ce
GdOI : 2% Ce
Br
Cl
h
LuOCl: 0.5% Ce
LuOBr: 0.5% Ce
LuOI : 1% Ce
Time (ns)

Fig. 2. (a–d) Room temperature X-ray excited emission spectra and (e–h) room temperature X-ray excited decay curves of select cerium-activated REOX scintillators.

Cerium-activated materials are expected to exhibit doublet emission peaks and exponential decays that correspond to transitions from the 5d configuration to the two terminating levels of the 4f configuration of Ce^{3+}: $^2F_{7/2}$ and $^2F_{5/2}$. Of the sixteen REOX materials, ten exhibit such signature cerium luminescence upon doping. Details are discussed below.

3.2.1. Oxyfluorides-REOF: Ce^{3+}

The REOF: Ce^{3+} materials do not exhibit cerium characteristic scintillation properties. Their scintillation light yields are low, and their emission peak intensities are either negligible or lack discernible cerium doublets. Moreover, the decay curves obtained from pulsed X-ray measurements are non-exponential with decay times ≥80 ns.

3.2.2. Oxychlorides-REOCl: Ce^{3+}

The yttrium and gadolinium oxychlorides show typical cerium emission and decay curves under X-ray excitation. Fig. 2(a) and (e) contain the emission spectrum and decay curve, respectively, of YOCl: 1% Ce^{3+}, the concentration exhibiting the highest light yield of the cerium-doped yttrium oxychloride samples. This material emits as a broad unresolved doublet covering 330–490 nm with maximum at 380 nm. It displays an exponential decay of 20 ns for 83% of its scintillation light. The remainder of the decay has lifetimes >1 μs.

Fig. 2(c) and (g) contains the emission spectrum and decay curve, respectively, of GdOCl: 0.5% Ce^{3+}, the concentration displaying the highest light yield of the cerium-doped gadolinium oxychloride samples. It emits as a broad unresolved doublet from 340 to 500 nm with maximum at 400 nm. Its decay curve reveals two major decay components: one at 25 ns for 63% of its scintillation light, and the other at 76 ns for 27% of its light. A slow rise time of 6 ns is evident in this material (see inset in Fig. 2(g)).

The LaOCl: Ce^{3+} materials exhibit atypical cerium scintillation under X-ray excitation. They emit as broad unresolved peaks in the range of 350–750 nm with maxima of 420 nm (Fig. 2(b)). Although the photoluminescence excitation spectra of each LaOCl: Ce^{3+} material shows cerium incorporation, their scintillation decay curves are non-exponential and slow; see Fig. 2(f). The LaOCl: 2% Ce^{3+} material, which has the highest light yield, displays a 17 ns decay component indicative of cerium; however, the majority of the decay has lifetimes ≥100 ns.

Broad asymmetric peaks with maxima of 380 nm are observed in the undoped and cerium-doped LuOCl materials (Fig. 2(d)). The intensity of this emission decreases as the concentration of cerium increases. Likewise, both the undoped and cerium-doped LuOCl materials exhibit non-exponential scintillation decay curves and have decays >300 ns. These characteristics are inconsistent with typical cerium activation.

3.2.3. Oxybromides-REOBr: Ce^{3+}

All four oxybromides exhibit cerium doublet emission and exponential decay curves upon doping. For the optimal cerium concentrations, their emission peaks range from 400 to 445 nm, and their major decay components have lifetimes ranging from 1 to 30 ns for ≥56% of their scintillation light.

The YOBr: 1% Ce^{3+} material exhibits the highest light yield found for the YOBr: Ce^{3+} samples and for all the yttrium oxyhalides. Fig. 2(a) presents the emission spectrum for this material. It emits as a doublet in the range of 380–520 nm with maxima at 400 and 445 nm. At all cerium concentrations studied, the intensity of the higher energy peak (i.e., the 400 nm peak) is reduced. An exponential decay of 25 ns dominates the decay curve accounting for 76% of the light (Fig. 2(e)). A second decay component of 59 ns is observed for 17% of the light.

The LaOBr: Ce^{3+} materials exhibit broad unresolved emission occurring at 370–600 nm with maxima that shifts from 420 to 430 nm as the concentration of cerium increases to 10 mol%. Abnormally fast decay components at 1, 4, and 13 ns are observed at all concentrations. LaOBr: 1% Ce^{3+} produces the greatest light yield of all the lanthanum oxybromides and has a peak maximum at 425 nm (Fig. 2(b)).

The 0.5% Ce^{3+}-doped GdOBr material displays the highest light yield of all the REOX materials with a relative luminosity, *RL*, of 48% of $LaBr_3$: 5% Ce^{3+}. It emits as a doublet between 380 and 520 nm with maxima at 405 and 445 nm. Each GdOBr: Ce^{3+} material displays exponential decays of 26–30 ns for >60% of their scintillation light. An additional decay component in the range of 60–95 ns is observed as well for samples with cerium concentrations >0.5%. The inset in Fig. 2(g) displays the observed slow rise time of 10 ns for GdOBr: 0.5% Ce^{3+}.

The LuOBr: 0.5% Ce^{3+} material exhibits the greatest light yield of all the lutetium oxyhalides. Its cerium doublet emission occurs from 375 to 520 nm with peak maxima at 405 and 445 nm. Like YOBr: Ce^{3+}, the intensity of the high energy peak is reduced in each LuOBr: Ce^{3+} material. Two major decay components are observed in this material: one at 25 ns for 56% of the light and the other at 73 ns for 10%. The remainder of the decay has lifetimes >200 ns.

3.2.4. Oxyiodides-REOI: Ce^{3+}

All four cerium-doped rare earth oxyiodides exhibit characteristic cerium emission and exponential decay components. They display emission peaks between 430 and 480 nm and have decay components with lifetimes of 20 and 24 ns for ≥67% of their light yields.

The yttrium and lutetium oxyiodides have optimal light yields at 1% doping. The X-ray excited emission spectra of these two materials are shown in Fig. 2(a) and (d). Both display doublet emission at 400–560 nm with maxima at 430 and 480 nm. The decay curves of YOI: Ce^{3+} and LuOI: Ce^{3+} are concentration dependent. At concentrations ≤2%, they exhibit exponential decays of 20–26 ns for >80% of their light. At 5% and 10% doping, components with lifetimes ranging from 4 to 17 ns make larger contributions to the overall decay curve. These faster decays are accompanied by lower light yields. The scintillation decay curves of YOI: 1% Ce^{3+} and LuOI: 1% Ce^{3+} are included in Fig. 2(e) and (h).

Of the lanthanum oxyhalides, LaOI: 2% Ce^{3+} exhibits the greatest light output. This trend was predicted by Chaudhry et al. [32]. It exhibits broad unresolved emission from 400 to 650 nm with peak maximum at 470 nm. Pulsed X-ray measurements of this material reveal an exponential decay component of 23 ns for 86% of its scintillation light.

The GdOI: 2% Ce^{3+} material displays the highest light yield of the cerium-doped gadolinium oxyiodides. It exhibits doublet emission at 400–560 nm with maxima at 440 and 470 nm and an exponential decay component of 23 ns for 67% of its scintillation light.

4. Discussion

4.1. Cerium-activated scintillation

4.1.1. (Y)(Gd)OCl: Ce^{3+}, REOBr: Ce^{3+}, and REOI: Ce^{3+}

The yttrium and gadolinium oxychlorides, and all the oxybromides and oxyiodides, exhibit characteristic cerium scintillation. As shown in Fig. 2(a–d), the emission peaks increase in wavelength going from Cl to I in each rare earth family. The oxychlorides emit as broad unresolved doublets with maxima at 380 and 400 nm for YOCl: Ce^{3+} and GdOCl: Ce^{3+}, respectively. The oxybromides emit as doublets with peaks in the 400–445 nm range. The oxyiodides emit as doublets with peaks in the 430–480 nm range. The positions of the emission peaks are independent of cerium concentration except those of LaOBr: Ce^{3+}. As the concentration of cerium increases from 0.5% to 10%, the peak maxima of LaOBr: Ce^{3+} shifts from 420 to 430 nm. Buchanan et al. [13] observed a broad emission peak with maximum of ~450 nm under electron beam irradiation for LaOBr: 1% Ce^{3+}, and Blasse et al. [12] observed a maximum of 438 nm under UV and cathode ray excitation for LaOBr: 1–2% Ce^{3+}.

The decay curves of the cerium-activated scintillators are presented in Fig. 2(e–h). Each material exhibits characteristic cerium decays of 20–30 ns. Several of the cerium-doped REOX materials also display major decay components (>10% of the curve) in the range of 45–95 ns. Using room temperature pulsed X-ray measurements, we attempt to explain the origins of these decays.

The GdOCl: Ce^{3+} and GdOBr: Ce^{3+} materials display slow rise times and decay components at each concentration of cerium. These features are common in cerium-doped gadolinium materials and originate from the transfer of Gd^{3+} luminescence to Ce^{3+} centers [33] and [34]. The YOBr: Ce^{3+} and LuOBr: Ce^{3+} materials display reduced intensities in their high energy peaks and slower decay components. These features suggest reabsorption processes similar to those reported in $CeBr_3$ and BaF_2: Ce^{3+} [35] and [36]. For all samples shown in Fig. 2, there are additional slow components (lifetimes>95 ns) in the decay curves that could be the result of delayed energy transfer to cerium.

Abnormally fast, exponential decays (lifetimes<20 ns) are observed in cerium-doped LaOBr, YOI, and LuOI. The LaOBr: Ce^{3+} materials exhibit decays of 1, 4, and 13 ns for all cerium concentrations studied. These decays could be the result of thermally induced quenching mechanisms at room temperature. Such quenching has been observed in LaI_3: Ce [2] and has been attributed to cerium 5d levels close to the conduction band of the host. The fast decay times observed at high concentrations in cerium-doped YOI, and LuOI are accompanied by decreased light yields. This indicates quenching of the luminescence due to increased Ce^{3+}–Ce^{3+} interactions [37], i.e., concentration quenching.

4.1.2. LaOCl: Ce^{3+}

Room temperature photoluminescence spectra of the LaOCl: Ce^{3+} materials show two cerium 5d excitation peaks at 280 and 315 nm and a 415 nm emission peak; on the other hand, under X-rays, a 420 nm broad emission peak with underlying emission up to 750 nm is observed. The excitation and emission spectra indicate that LaOCl is activated by cerium, and a decay component of 17 ns is observed in the scintillation decay. However, the overall decay curve is non-exponential and has major decay components ≥100 ns for each LaOCl: Ce^{3+} material. Likewise, under electron beam irradiation, Buchanan et al. [13] observed a decay time of 100 ns for LaOCl: 1% Ce^{3+}. The slow scintillation observed by us and Buchanan could be linked to the underlying emission at 500–750 nm noted in our X-ray excited emission spectra. An emission peak maximum of 360 nm was observed for LaOCl: Ce^{3+} by Blasse and Bril [12] under UV and cathode ray excitation. However, we suggest this emission matches that of $LaCl_3$: Ce^{3+}, an easily made by-product.

4.2. Non-cerium scintillation

4.2.1. REOF: Ce^{3+}

The X-ray excited emission and decay curves of the oxyfluorides are not consistent with cerium signature emission. This can be explained by the large band gaps expected for these materials. First-principle calculations reveal large Ce^{3+} 4f-valence band gaps for YOF: Ce^{3+} and LaOF: Ce^{3+}. These gaps reduce the probability of cerium to trap holes, thereby decreasing the probability of cerium scintillation [32]. As a result, the luminescence observed under X-rays could be attributed to intrinsic luminescence from the host instead of cerium. This may also explain the non-cerium scintillation of GdOF: Ce^{3+} and LuOF: Ce^{3+}.

4.2.2. LuOCl: Ce^{3+}

The LuOCl: Ce^{3+} materials do not demonstrate cerium characteristic emission under X-rays. It is unclear from room temperature optical excitation and emission measurements whether LuOCl is activated by cerium. LuOCl: Ce^{3+} emission under UV and X-ray excitation has low yield and is similar to emission observed from undoped LuOCl. This emission could be attributed to intrinsic processes from the host that were not further explored in this study.

4.3. Structural influences

These REOX compounds crystallize into one of three structure types. The oxychlorides, oxybromides, and oxyiodides of yttrium, lanthanum, and gadolinium, as well as lutetium oxybromide and oxyiodide, have two-dimensional layered tetragonal structures (space group P4/nmm, PbFCl type) [20] and [9]. The yttrium, lanthanum, and gadolinium oxyfluorides and the lutetium oxychloride crystallizes in the same three-dimensional rhombohedral structure (space group R-3m) [21], [22], [23] and [27]. Lastly, the lutetium oxyfluoride crystallizes three-dimensionally in the monoclinic space group $P2_1/c$ [24].

Previous studies of the structural influences on luminescence suggest that the delocalization of the excited electrons in three-dimensionally coupled d-orbitals accounts for the quenching of

photoluminescence in many phosphors [38] and [39]. The more isolated the excited state structure, the less likely the excited electron will find quenching centers; therefore, luminescence has a better chance of occurring in compounds with less dimensionality.

In our study of the REOX compounds, we found that the oxyhalides that crystallize in the two-dimensional tetragonal structure are activated by trivalent cerium and show fast scintillation. One exception is LaOCl: Ce^{3+}, whose overall scintillation is abnormally slow, possibly due to competing emission. The oxyfluoride and LuOCl materials have three-dimensional structures, which could contribute to their lack of fast, exponential decays, and efficient cerium luminescence upon doping. In particular, Rabatin [14] also observed "different" emission in LuOCl: Ce^{3+} relative to LuOBr: Ce^{3+} and attributed it to structural dissimilarities.

5. Conclusions

The room temperature scintillation properties were obtained of cerium-doped rare earth oxyhalides following the formula REOX (RE=Y, La, Gd, and Lu; X=F, Cl, Br, and I). Of these materials, YOCl: Ce^{3+}, GdOCl: Ce^{3+}, and all the oxybromides and oxyiodides show typical cerium-activated characteristics in their scintillation light. Of these materials, three stand out as displaying attractive combinations of densities (5–7 g/cm^3), Z_{eff} (36–54), and moderate light yields: YOBr: 1% Ce^{3+}, LaOI: 2% Ce^{3+}, and GdOBr: 0.5% Ce^{3+}. They also display cerium exponential decays of 27, 24, and 30 ns, respectively. Unfortunately, these materials may be difficult to grow as large crystals since they have layered structures.

In addition, the rare earth oxychlorides and oxybromides were found to be less hygroscopic than their rare earth halide counterparts. This indicates that not only can oxyhalides be efficient cerium-activated hosts, they may also be more stable than their corresponding halides. Furthermore, we observed that the cerium activation of these rare earth oxyhalides may be linked to the structural dimensionality of the host.

Disclaimer

Acknowledgments

The authors would like to thank Marvin Weber for his invaluable input in the writing of this manuscript and all the members of the Department of Radiotracer Development and Imaging Technology at LBNL. In addition, we want to thank Matthias Klintenberg for his suggestions to investigate several of these materials. This work was supported by the US Department of Homeland Security and was carried out at the Lawrence Berkeley National Laboratory under US Department of Energy Contract no. DE-AC02-05CH11231.

References

[1] S.E. Derenzo, M. J. Weber, E. D. Bourret-Courchesne, M. K. Klintenberg, Nucl. Instr. and Meth. A 505 (2003) 111-117.
[2] A. Bessiere, P. Dorenbos, C.W.E. Van Eijk, K. Kramer, H.U. Gudel, C. de Mello Donega, A. Meijerink, Nucl. Instr. and Meth. A 537 (2005) 22-26.
[3] O. Guillot-Noel, J.T.M. de Haas, P. Dorenbos, C.W.E. van Eijk, K. Kramer, H.U. Gudel, J. Lumin. 85 (1999) 21-35.
[4] W.W. Moses and S.E. Derenzo, Nucl. Instr. and Meth. A 299 (1990) 51-56.
[5] E.V.D. van Loef, P. Dorenbos, C.W.E. van Eijk, K. Kramer, H.U. Gudel, Appl. Phys. Letters 79 (2001) 1573-1575.
[6] E.V.D. Van Loef, P. Dorenbos, C.W.E. Van Eijk, K. Kramer, H.U. Gudel, Nucl. Instr. and Meth. A 486 (2002) 254-258.
[7] A.J. Wojtowicz, M. Balcerzyk, E. Berman, A. Lempicki, Phys. Rev. B 49 (1994) 14880-14895.
[8] K. Shah, J. Glodo, M. Klugerman, W. Higgins, T. Gupta, P. Wong, W.W. Moses, S.E. Derenzo, M.J. Weber, P. Dorenbos, IEEE Trans. Nucl. Sci. 51 (2004) 2302-2305.
[9] E.V.D. Van Loef, P. Dorenbos, C.W.E. Van Eijk, K. Kramer, H.U. Gudel, Nucl. Instr. and Meth. A 496 (2003) 138-145.
[10] P.R. Menge, G. Gautier, A. Iltis, C. Rozsa, V. Solovyev, Nucl. Instr. and Meth. A. 579 (2007) 6-10.
[11] J.T.M. d. Haas, P. Dorenbos, IEEE Trans. Nucl. Sci. 55 (2008) 1086-1092.
[12] G. Blasse, A. Bril, J. Chem. Phys. 47 (1967) 5139-5145.
[13] R.A. Buchanan, T.G. Maple, A.F. Sklensky, I. Lockheed Missiles & Space Company, U.S. Patent No. 4,297,584: Lockheed Missiles & Space Company, Inc. (1981) 65-80.
[14] J. Rabatin, J. Electrochem. Soc. 129 (1982) 1552-1555.
[15] D. Starick, S. I. Golovkova, A. M. Gurvic, J. Lumin. 40-41 (1988) 199-200.
[16] J. Holsa, M. Lahtinen, M. Lastusaari, J. Valkonen, J. Viljanen, J. Solid State Chem. 165 (2002) 48-55.
[17] J. Lee, Q. Zhang, F. Saito, J. Solid State Chem. 160 (2001) 469-473.
[18] S.E. Derenzo, M.S. Boswell, E.D. Bourret-Courchesne, R. Boutchko, T.S. Budinger, A. Canning, S.M. Hanrahan, M. Janecek, Q. Peng, Y.D. Porter-Chapman, J. Powell, C.A. Ramsey, S.E. Taylor, L.-W. Wang, M.J. Weber, D.S. Wilson, IEEE Trans. Nucl. Sci. 55 (2008) 1458-1463.
[19] S.E. Derenzo, M.J. Weber, W.W. Moses, C. Dujardin, IEEE Trans. Nucl. Sci. 47 (2000) 860-864.
[20] PDF4+ Powder Diffraction File, Newton Square, PA, USA: International Centre for Diffraction Data (2007).
[21] A.W. Mann, D. J.M. Bevan, Acta Crystallogr. B 26 (1970) 2129-2131.
[22] W.H. Zachariasen, Acta Crystallogr. 4 (1951) 231-239.
[23] S. Kirik, L. Solovyov, G. Korolev, Inst. of Chemistry, Academy of Sciences, Krasnoyarsk, Russia, ICDD Grant-in-Aid (1997).
[24] A. Taoudi, J.P. Laval, B. Frit, Mater. Res. Bull. 29 (1994) 1137-1147.
[25] W.H. Zachariasen, Acta Crystallogr. 2 (1949) 388-390.
[26] L.G. Sillen, A.L. Nylander, Svensk Kemisk Tidskrift 53 (1941) 367-372.
[27] L. Brixner, J. Lumin. 26 (1981) 1-19.
[28] H.J. Limburg, J. Hoelsae, P. Porcher, G. Herzog, D. Starick, H. Wulff, J. Solid State Chem. 98 (1992) 404-414.

[29] S. Putilin, E. Antipov, Moscow State Univ. Russia. ICDD Grant-in-Aid (1995).
[30] G. Meyer, Institut fur Anorganische Chemie, Universitat Hannover, Hannover, Germany. ICDD Grant-in-Aid (1990).
[31] R.D. Shannon, Acta Cryst. A32 (1976) 751-767.
[32] A. Chaudhry, A. Canning, R. Boutchko, Y.D. Porter-Chapman, E. Bourret-Courchsne, S.E. Derenzo, IEEE Trans. Nucl. Sci. 56 (2009) 949-954.
[33] H. Suzuki, T.A. Tombrello, C.L. Melcher, C.A. Peterson, J.S. Schweitzer, Nucl. Instr. and Meth. A. 346 (1994) 510-521.
[34] Y.D. Porter-Chapman, E.D. Bourret-Courchesne, G. Bizarri, M.J. Weber, S.E. Derenzo, IEEE Trans. Nucl. Sci. 56 (2009) 881-891.
[35] W. Drozdowski, P. Dorenbos, A.J.J. Bos, G. Bizarri, A. Owens, F.G.A. Quarati, IEEE Trans. Nucl. Sci. 55 (2008) 1391-1396.
[36] W. Drozdowski, A.J. Wojtowicz, Nucl. Instr. and Meth. A. 486 (2002) 412-416.
[37] P. Lecoq, A. Annenkov, A. Gektin, M. Korzhik, C. Pedrini, Inorganic Scintillators for Detector Systems, New York City, NY: Springer-Verkag Berlin Heidelberg (2006) 94.
[38] G. Blasse, Prog. Solid St. Chem. 18 (1988) 79-171.
[39] A.M. Srivastava, J.F. Ackerman, J. Solid State Chem. 134 (1997) 187-191.